大阪公立大学
Osaka Metropolitan University
学術情報リポジトリ

Visualization of High Speed Flow using Aluminium Flakes as Tracers

メタデータ	言語: English 出版者: 公開日: 2010-04-05 キーワード (Ja): キーワード (En): 作成者: Sugimoto, Akiya, Matsumoto, Ken, Nakamura, Kyo, Nakamura, Kozo メールアドレス: 所属:
URL	https://doi.org/10.24729/00008812

Visualization of High Speed Flow using Aluminium Flakes as Tracers

Akiya SUGIMOTO*, Ken MATSUMOTO**, Kyô NAKAMURA***
and Kôzô NAKAMURA*

(Received June 14, 1971)

In this paper, an experimental method is written about the three dimensional analysis of air flows. The merits of the method are that the three dimensional data can be obtained from a photograph of tracers, and that the air flow of quite high speed can be analyzed.

The air flows are examined in an abrupt bend and a channel with sudden contraction. The results show that the traces of flakes are in fairly good agreement with the flow lines of the air; further, the deviations of traces from the flow lines are made clear. The way of the three dimensional analysis is also tried and discussed.

1. Introduction

For the flow of very low speed, various methods[1),2)] can be adaptable to the purpose of flow visualization; however, the number of available methods is a few for high speed flows. The present method is adaptable to the air flow slower than about 50 m/s; moreover, the flow of the higher speed could be examined after a few improvements. The other merit is that the three dimensional data can be obtained from a photograph of tracers, though an ordinary photograph offers two dimensional data[2)]. The principle of the three dimensional analysis depends on the indirect measurement of perspective distances, which are calculated from the diameters of the circles of confusion.

The present equipment had been developed for the purpose of the visualization of complicated flows in air turbines; therefore, the compliance of traces in the flows was essential. The deviations of the traces from the flow lines are very small in the range of the present experiments. However, it is necessary for the estimation of exact flow lines from the traces of flakes that the coefficient of entrainment K (defined by Eq. 1) is known. The value of K measured in the experiments is larger than 2500 s^{-1}, and the average value is about 7000 s^{-1}.

2. Experimental equipment and methods

The photographic method needs the tracers, the light sources, the optical system and the controll system.

* Department of Mechanical Engineering, College of Engineering.
** Graduate Student, Department of Mechanical Engineering, College of Engineering.
*** Student, Department of Mechanical Engineering, College of Engineering.

2.1 Tracer

Favourable properties for the tracer are as follows: the light reflection is strong, the frontal area is wide and the weight is light. An aluminium flake is suitable for these properties; among all, the first one is sufficiently satisfied, and the second and third ones are deduced from the following equation[1],

$$dv/dt = C_d \rho_a (u-v)^2 A/2m = K(u-v)\,, \qquad (1)$$

where v is the velocity of the flake, u the velocity of the air, t the time, C_d the drag coefficient, ρ_a the density of the air, A the frontal area of the flake, m the mass of the flake and K the coefficient of entrainment. It is preferable for the decrease of the deviation between the flow lines and the traces of the flakes that the value of K is large, that is, the size of the flake is small.

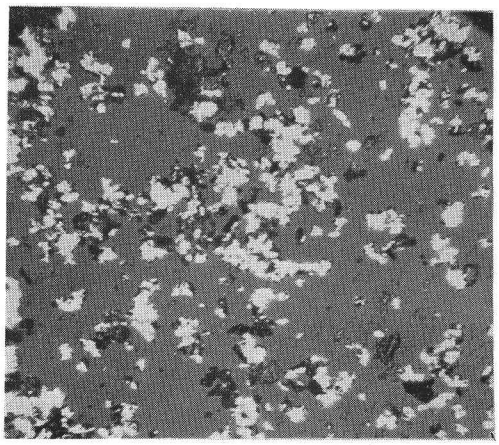

0 50 100 (μ)

Photo. 1. Flakes.

In Photo. 1, the shapes of the aluminium flakes used in the experiments through the microscope are illustrated. The sizes of the flakes are almost under 10 μ (sometimes, the flakes get together in the photograph); therefore, it can be expected that the deviation is not too large.

2.2 Light sources

Many investigators[3),4)] took photographs of small particles by means of double exposures. The merit of these methods is that the particles of high speed can be photographed. The following conditions are convenient to take a photograph of flakes which are drifting in the air flow of high speed: i) the time interval between two flashes is controlled in an arbitrarily fixed time, ii) the time durations of the flashes are very short for taking the sharp photograph, iii) when one of the flashes has a little longer duration, the distinction of the pair of the images can be easy.

Fig. 1 shows the circuit of the light sources. The duration of the second light can be approximately estimated from the following equations,

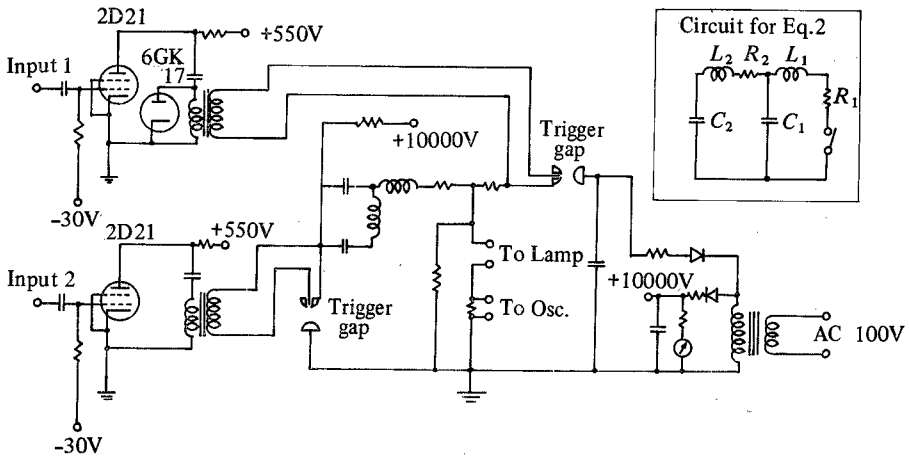

Fig. 1. Light source.

$$\left.\begin{aligned} &L_1\left(\frac{d^2Q_1}{dt^2}+\frac{d^2Q_2}{dt^2}\right)+R_1\left(\frac{dQ_1}{dt}+\frac{dQ_2}{dt}\right)+\frac{Q_1}{C_1}=0\,,\\ &L_2\frac{d^2Q_2}{dt^2}+R_2\frac{dQ_2}{dt}+\frac{Q_2}{C_2}-\frac{Q_1}{C_1}=0\,,\end{aligned}\right\}\qquad(2)$$

where t is the time, Q_1 and Q_2 are the electric charges of the condencers C_1 and C_2, respectively, and the other notations are written in Fig. 1. The solutions and the experimental results are shown in Appendix I.

The circuit for the time delay of the second flash from the first flash is shown in Fig. 2. The delay time is varialbe in the range of 2×10^{-6} to 15×10^{-3}s.

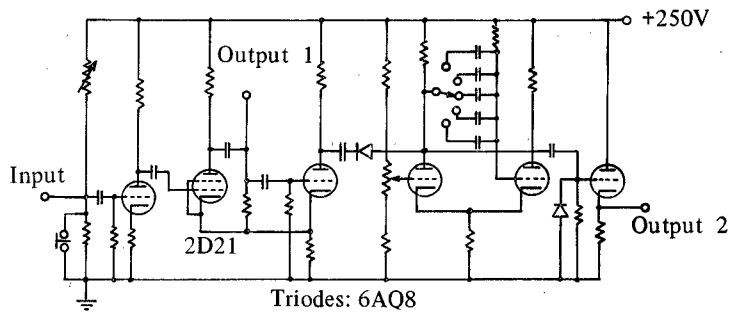

Fig. 2. Time delay circuit.

2.3 Optical system

When the photograph of a small particle such as the flake is taken, the large magnification must be demanded to make picture distinct. However, the large magnification

is not always necessary to take a photograph of the image of the circle of confusion. If the magnification of the camera lens is larger than 3, the total magnifying power can be 100 by the aid of a projector. This value is enough to make the distinct image. The relation between the diameter of the circle of confusion and the distance from an object to the focal plane of the object space was written in Reference 5. The size of the object is very small in the present case; therefore, the relation can be expressed approximately as follows:

$$s = aD, \tag{3}$$

where s is the distance from the object to the focal plane, D the diameter of the circle of confusion and a the constant determined from the optical system. When s is minus, $-s$ is approximately equal to aD. Consequently, the mistake of the sign may occur on the analysis of the images. The mistake can be avoided by means of the illumination

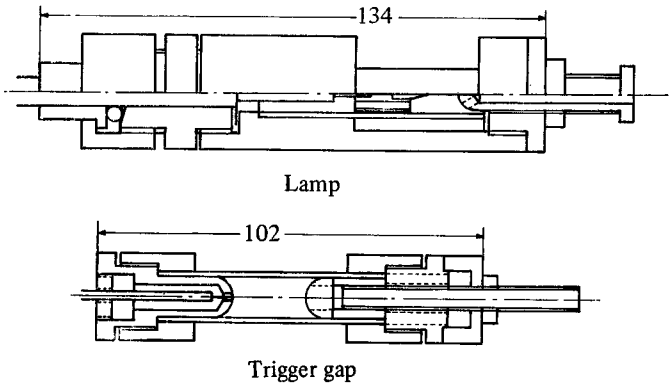

Fig. 3. Lamp and Trigger gap (Dimensions in mm).

of only the plus side field of s. For this purpose, the lights are made into the thin beam through a condenser lens, and they illuminate the tracers from the direction transvers to the axis of the camera lens (the width and depth of the light beam are about 10 mm and 7 mm, respectively). The lamp of the light and the trigger gaps are drawn in Fig. 3.

Thus, we can see the perspective distance of an image on the picture from the diameter of it, that is, the three dimensional measurement is possible.

2.4 Controll system and experimental methods

The diagram of the equipment is illustrated in Fig. 4. The tracer strewing device, the camera shutter and the light sources are controlled with the circuit drawn in Fig. 5 and the pneumatic devices (solenoid air valves and air releases).

In Fig. 4, the air premixed with the tracers enters into the channel and is sucked out by a blower. Since the camera shutter is opened, the lights illuminate the tracers. These procedures are controlled by the circuit as mentioned before (see Fig. 5). After the photograph is taken and the film is developed, the film is projected to a screen with magnifying 100 times the object and it is examined.

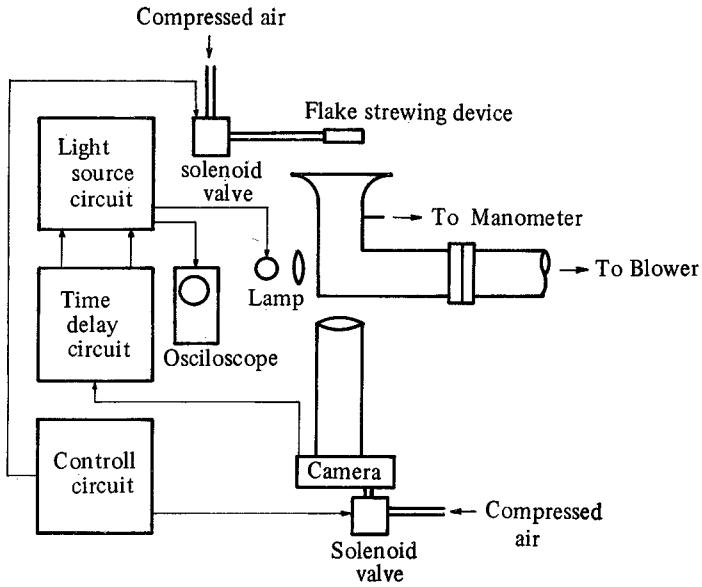

Fig. 4. Diagram of equipment.

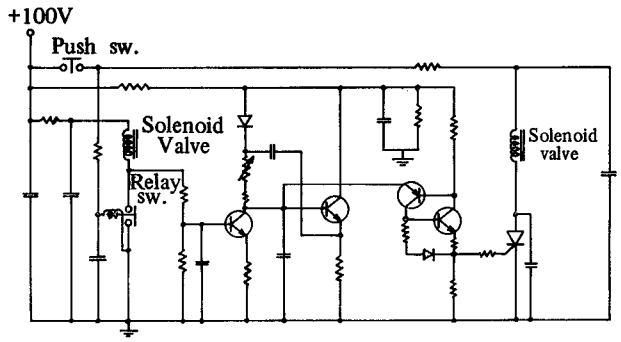

Fig. 5. Controll circuit.

In Photo. 2, circles are images by the first light; distorted ellipses are images by the second light. The diameter of a circle and the minor axis of an ellipse can be used to calculate s from Eq. 3. On the production of the major axis of an ellipse, there is a circle paired with the ellipse; therefore, the selection of the pair is an easy task which is accompanied with no misjudgement. (For particulars, see Appendix I).

The time interval between two lights is measured by using the osciloscope (see Appendix I). The three dimensional velocity components of the tracer are calculated from the sizes and the positions of the images of the tracer and the time interval between two lights.

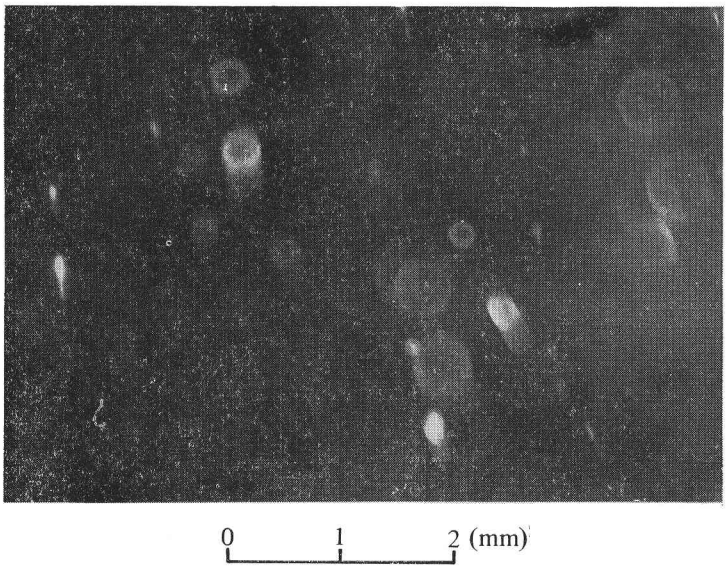

Photo. 2. Tracers in the channel.

3. Results and discussion

Fig. 6*a* shows the test channel, in which tracers are photographed from the two directions. Though the movement of the tracer which runs only toward the direction of the axis of the camera lens is not detected on account of the overlap of the images of the tracer, the three dimensional movement can be measured on a photograph except such a case. Fig. 7*a* and 7*b* illustrate the velocities v and the directions α of the tracers which are measured on the line $A-A'$ in Fig. 6*a* from the two directions. In

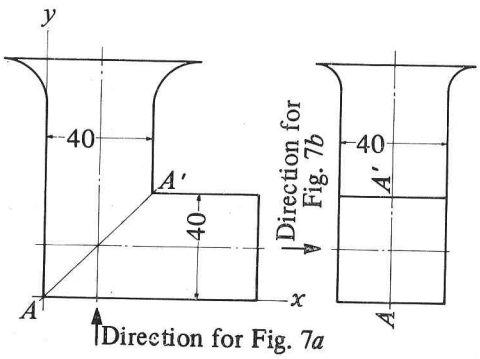

Fig. 6a. Channel (All dimensions in mm).

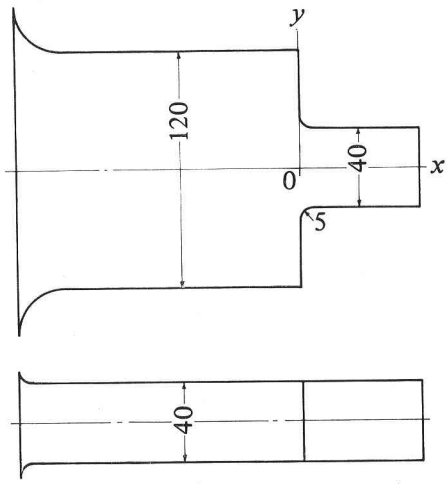

Fig. 6b. Channel (All dimensions in mm).

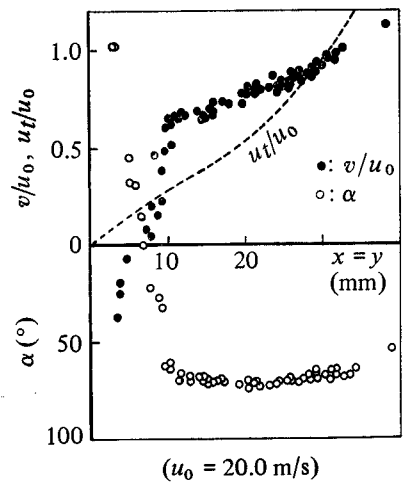

Fig. 7a. Velocity and direction. (α: Flow direction of tracers)

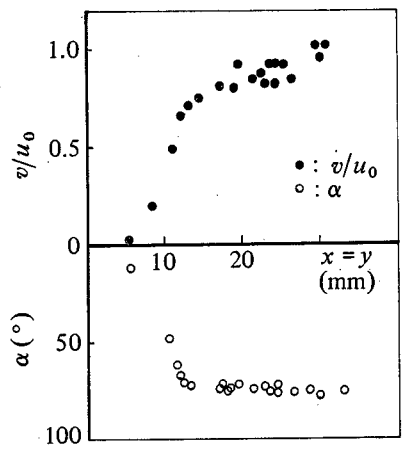

Fig. 7b. Velocity and direction.

Fig. 7*a*, u_t is the theoretically calculated velocity (see Appendix II), and u_t and the theoretically calculated angle $\alpha_t(\alpha_t=45°)$ are quite different from those obtained in the experiments. However, the results in Fig. 7*a* show good agreement with those in Fig. 7*b*, that means, the three dimensional measurement of the movement of the tracer can be done almost perfectly from either of the two directions.

The compliance of the velocity of the tracer to that of the flow can be appreciated from the value of the coefficient of entrainment K. K can be derived from the terminal velocity of the tracer. However, the measurement of the terminal velocity should require a strict technique[1]. In the present experiments, the velocities of the tracers and the air were measured along the center line of the duct shown in Fig. 6*b*. Strictly speaking, K is not constant and Eq. 1 is an approximate equation. The influence of the acceleration which causes to the approximation is small and it can be neglected[6,7]. K is assumed as constants in the range of the experiments.

The velocity of the flow u is expressed as a function of the distance x, and Fig. 8 shows the velocities of the flow and the tracers. Since the derivative of v with respect to t is equal to $v\mathrm{d}v/\mathrm{d}x$, the derivative of v with respect to x is written as

$$\frac{\mathrm{d}v}{\mathrm{d}x}=K\left(\frac{u}{v}-1\right). \tag{4}$$

K can be calculated from Eq. 4 by using numerical computation. In Fig. 9, the numerical differentiation of the data is not used, but the numerical integration (Runge-Kutta method) is applied to the calculation after estimating the value of K. K is larger than 2500 s^{-1} and the average value is about 7000 s^{-1} from Fig. 8 and 9. The values of K in the experiments are in fairly good agreement with those written in Reference 1, in which the trial calculation (K is 15000 s^{-1} for a 4 μ aluminium flake having 1 μ thick) and the results by Bourot (K is in the range of 2500 to 33000 s^{-1}) are written.

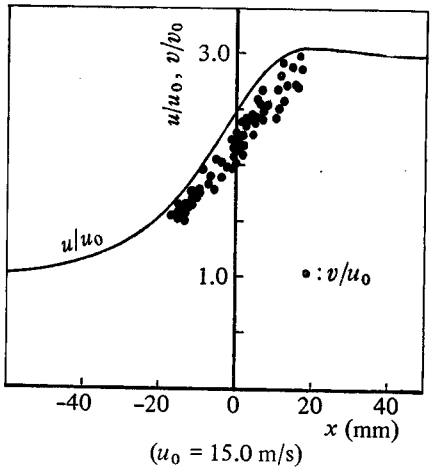

Fig. 8. Velocities of tracers v.

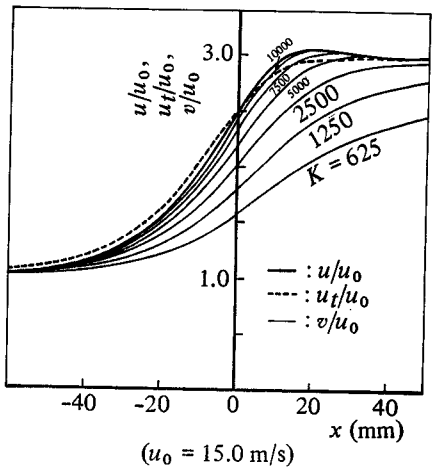

Fig. 9. Air velocity and calculated velocilies.

When tracers are used for the measurement of the velocity of an air stream, the velocity of the tracer is the value of the first approximation of the air velocity. Assuming K from the previously measured values, we can calculate the second approximation of the air velocity from the data. For example, u is expressed from Eq. 1 as follows:

$$u = v\left(1 + \frac{1}{K}\frac{\mathrm{d}v}{\mathrm{d}x}\right),$$

where $\mathrm{d}v/\mathrm{d}x$ can be calculated by using numerical differentiation from the difference of v with respect to x. Of cource, we can estimate the error from $(1/K)(\mathrm{d}v/\mathrm{d}x)$, when the correction mentioned above is curtailed.

4. Conclusions

A photographic method which gives us the three dimensional data of flow lines of quite high speed is developed and tested. The results show that the three dimensional distribution of air velocities can be obtained from a photograph taken by means of this technique and that the coefficient of entrainment measured here is useful for the estimation of the compliance of tracers.

The experiments were attempted to examine the equipment which was made for an investigation of the flow in air turbines. Further, the method could be used for various purposes.

References

1) R.W. Ladenburg and others, Pyhsical Measurements in Gas Dynamics, p 142, Geoffrey Cumblerege Oxford Univ. Press, London (1955).
2) J.O. Hinze, Turbulence, p. 126, McGraw-Hill Book Co. Inc. London (1959).
3) J.L. York and H.E. Stubbs, Trans. ASME, **74**, 1157 (1952).

4) J.A. Bolt and A.J. Erickson, Trans. ASME, **78**, 609 (1956).
5) A. Sugimoto, Bull. of Univ. of Osaka Pref., **A18**–2, 279 (1969).
6) R.G. Lunnon, Proc. Roy. Soc., **110A**, 302 (1926) and **118A**, 680 (1928).
7) R.R. Hughes and E.R. Gilliland, Chem. Engng. Progress, **48**–10, 497 (1952).
8) L.M. Milne-Thomson, Theoretical Hydrodynamics, p. 287, Macmillan & Co. Ltd. London (1968).

Appendix I

The solution of Eq. 2 is obtained through the Laplace transform as

$$Q = (A \sin \beta t + B \cos \beta t)e^{\alpha t} + Ce^{\gamma t} + De^{\delta t},$$

where Q is the electric charge of condensers (C_1 and C_2), t the time and A, B, C, D, α, β, γ and δ the constants.

The results of the numerical calculation are illustrated in Fig. 10. If a square wave is obtained, an image on a photograph becomes a symmetrically distorted ellipse for high speed flow. The waves in Fig. 10 are rather deformed squares and have many oscillations after main waves. Photo. 3 illustrates the wave of the first and second lights. The time duration of the first light is about 2 μs, and the first light has a fairly large wave close to the main wave. The second light flashes after the first one having the interval of about 46 μs. The duration of the second light is about 10 μs and the second light has also a

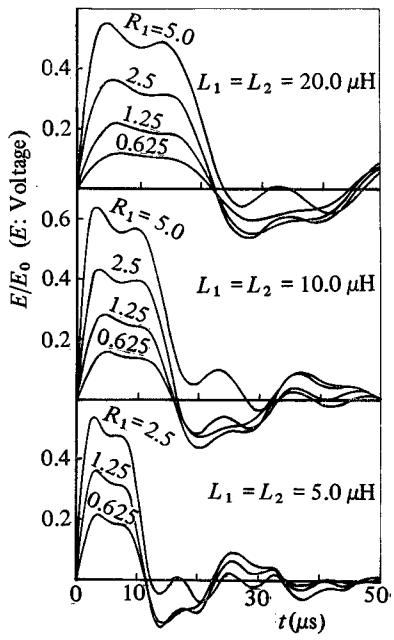

Fig. 10. Voltage of R_1.

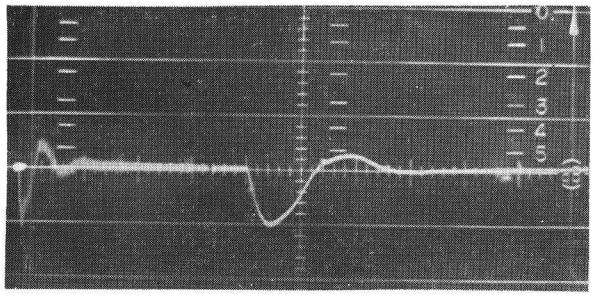

Photo. 3. Wave of lights.

fairly large wave just as the first one. The effect of these lights is seen in Photo. 2, that is, the third images exist close to the second images. Of cource, the proper damping resistance makes the third image extinct as shown in Fig. 10.

Appendix II

The Schwarz-Christoffel transformation for the channel shown in Fig. 6*a* is as follows:

$$\frac{dz}{d\zeta} = \frac{h}{\pi\zeta}\left(\frac{\zeta-1}{\zeta+1}\right)^{1/2}, \quad \frac{dw}{dz} = U\left(\frac{\zeta+1}{\zeta-1}\right)^{1/2}, \quad t = \left(\frac{\zeta-1}{\zeta+1}\right)^{1/2},$$

and the integration gives

$$z = \frac{h}{\pi}\left[\frac{1}{i}\log\left(\frac{1+it}{1-it}\right) - \log\left(\frac{1+t}{1-t}\right)\right] + h(1+i),$$

where z is the coordinate, ζ the coordinate, h the breadth, w the complex potential and

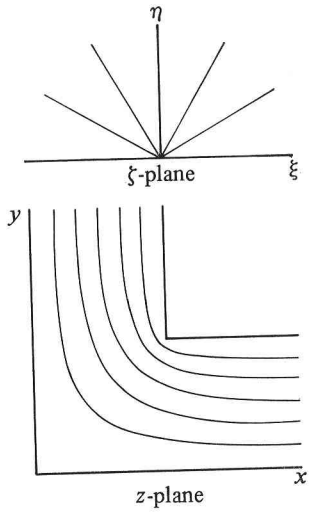

Fig. 11a. Flow lines by conformal mapping.

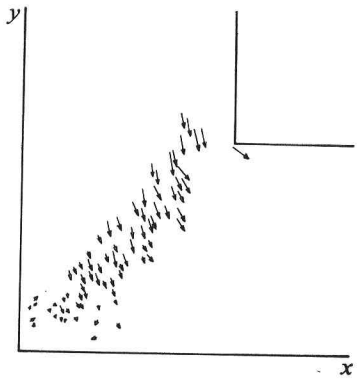

Fig. 11b. Traces.

U the velocity at $\eta = \infty$. The results are illustrated in Fig. 11*a*. The experimental results are shown in Fig. 11*b*, where the arrows denote the velocities of tracers (the lengths of the arrows corresponed to the speeds of the tracers).

The conformal mapping (as for the channel shown in Fig. 6*b* having no round at the corner of the neck) is described in Reference 8. The velocity of the flow u_t which is calculated by the conformal mapping is shown in Fig. 9. The theoretically calculated velocity is in good agreement with that of the experiments. The air flow has a contracted flow at the neck, and the effect of the contracted flow is well shown in Fig. 9 as the variation of the air velocity u and as the small discrepancy in the curves of u_t and u.